How far the zone of heat-induced transient block extends beyond the lesion during RF catheter cardiac ablation

How far the zone of heat-induced transient block extends beyond the lesion during RF catheter cardiac ablation

Juan J. Pérez [1], Enrique Berjano [1], Ana González-Suárez [2,3]

[1] *BioMIT, Department of Electronic Engineering, Universitat Politècnica de València, Valencia, Spain*
[2] *School of Engineering, University of Galway, Ireland,*
[3] *Translational Medical Device Lab, University of Galway, Ireland*

Corresponding author: Dr. Ana González-Suárez, Translational Medical Device Lab, 2nd Floor, Lambe Translational Research Facility, University College Hospital Galway, Ireland. Email: ana.gonzalezsuarez@nuigalway.ie

Funding details: Spanish Ministerio de Ciencia, Innovación y Universidades / Agencia Estatal de Investigación IMCIN/AEI/10.13039/501100011033 (Grant RTI2018-094357-B-C21).

Word count: 4,742
Running head: Transient block zone during RF cardiac ablation.

Conflict of interest: The authors have no conflicts to disclose.

Data availability: The data underlying this article will be shared on reasonable request to the corresponding author.

Abstract

Purpose: While radiofrequency catheter ablation (RFCA) creates a lesion consisting of the tissue points subjected to lethal heating, the sublethal heating (SH) undergone by the surrounding tissue can cause transient electrophysiological block. The size of the zone of heat-induced transient block (HiTB) has not been quantified to date. Our objective was to use computer modeling to provide an initial estimate.

Methods: We used previous experimental data together with the Arrhenius damage index (Ω) to fix the Ω values that delineate this zone: a lower limit of 0.1–0.4 and upper limit of 1.0 (lesion boundary). An RFCA computer model was used with different power-duration settings, catheter positions and electrode insertion depths, together with dispersion of the tissue's electrical and thermal characteristics.

Results: The HiTB zone extends in depth to a minimum and maximum distance of 0.5 mm and 2 mm beyond the lesion limit, respectively, while its maximum width varies with the energy delivered, extending to a minimum of 0.6 mm and a maximum of 2.5 mm beyond the lesion, reaching 3.5 mm when high energy settings are used (25W–20s, 500 J). The dispersion of the tissue's thermal and electrical characteristics affects the size of the HiTB zone by ±0.3 mm in depth and ±0.5 mm in maximum width.

Conclusions: Our results suggest that the size of the zone of heat-induced transient block during RFCA could extend beyond the lesion limit by a maximum of 2 mm in depth and approximately 2.5 mm in width.

Keywords: Cardiac ablation; computer modeling; mild hyperthermia; moderate heating; transient block.

1. Introduction

Radiofrequency (RF) catheter ablation (RFCA) is a minimally invasive technique that has been in use for more than 40 years and has become the standard for the treatment of many types of cardiac arrhythmias. During RFCA, RF current is applied through an ablation electrode on the catheter tip. RF current provokes that the temperature raises above 50 ºC in the myocardium around the electrode, resulting in cell death by denaturing both functional and structural proteins [1]. Although it is generally accepted that tissue temperatures ≥ 50 ºC in RFCA cause irreversible thermal injury [2], it is also known that hyperthermia-induced thermal damage is dependent not only on temperature but also on exposure time [1]. Both the 50 ºC isotherm and the damage index Ω have traditionally been used to estimate lesion size in computer modeling of RFCA [3]. The goal of RFCA is to eliminate the focus of the arrhythmia, i.e. the group of cells involved in the irregular heartbeat. The arrhythmia will remain if these cells are not affected and the ablation will not be successful. In practice, various circumstances can cause the process to fail, e.g. the focus might be too far from the electrode and the lesion might not be deep enough to be destroyed.

Hyperthermia-induced alteration of the electrophysiological activity of cardiac cells is not always an irreversible process, and the alterations may be hence transitory in the case of moderate hyperthermia (<50 ºC), e.g. reversible loss of excitability and transient block of electrical conduction [4–6]. In fact, it is reasonable to assume that the cells around the lesion have been subjected to moderate RFCA heating that has caused transient changes in their electrophysiological activity (see Fig. 1). In practice, the effects of ablation will be transient if the focus of the arrhythmia is subjected to moderate heating only.

While all the previous RFCA computer models focused on assessing the temperature

distributions and predicting lesion size [3], no previous computational or experimental study has so far focused on estimating the area of tissue subjected to sublethal heating capable of causing transient electrophysiological changes. Despite the limitations inherent in computational models, an initial estimation is certainly relevant scientific information with practical clinical implications. Our objective was therefore to use computer modeling to estimate how far the zone of heat-induced transient block extends beyond the lesion during RFCA.

2. Methods

2.1. Thermal injury model

Most RFCA studies that used computer modeling have estimated the lesion zone using either a lethal isotherm (50–55 ºC) or a mathematical function to take the 'thermal history' at each point in the tissue into account [3]. The most frequently used function models the tissue damage as an irreversible first-order chemical reaction, with the rate constant following the Arrhenius relationship [7], specifically, with the thermal injury index Ω, which relates the number of undamaged cells *C(0)* present before heating to the number of undamaged cells remaining at time *t,* indicated by *C(t)* as follows:

$$\Omega(t) = \ln(\frac{C(0)}{C(t)}) \quad (1)$$

This can be computed from the temperature *T* (in Kelvin) reached at each instant *t* (s) of the heating period (including the cooling period after the RF pulse):

$$\Omega(t,T) = \int_0^t Ae^{[-E_a/RT(\tau)]}d\tau \quad (2)$$

where A is the frequency factor, E_a is the activation energy, and R the universal gas constant (8.3143 J/mol·K). The values of A and E_a are particular for each tissue type and analyzed process. In previous modeling studies of RFCA, values of $A = 7.39\times10^{39}$ s^{-1} and $E_a = 2.577\times10^5$ J/mol were used to model the irreversible thermal damage and to estimate hence the lesion size. It was checked that these values provide a $\Omega = 1$ isoline more or less coincident with the 72 ºC isotherm for 5 s heating [8] and more or less coincident with the 55 ºC isotherm after 60 s of heating [2,9], which is in line with the experimental data. Lesion size can hence be calculated by considering all the points in the tissue at which $\Omega \geq 1$. Using Eq. (1), a value of $\Omega = 4.6$ is equivalent to 99% cell death probability, while a value of $\Omega = 1$ is equivalent to 63%. In the present study, we used the Arrhenius function to estimate the tissue area affected by a sublethal dose of thermal damage capable to cause a transient block in impulse conduction.

2.2. Modeling of the heat-induced transient block zone

As far as we know, only three experimental studies have measured temporary physiological changes in the myocardium associated with heating, including loss of excitability and conduction [4–6]. To estimate the tissue volume subjected to sublethal heating capable to cause transient block during RFCA, we first searched for the values of Ω of a thermal history (i.e. combinations of temperature and time) compatible with reversible loss of excitability and conduction. If the tissue is subjected to a constant temperature (T_H) for a specific time (t_H), Eq. (2) is greatly simplified and can be expressed as the following simple formula:

$$\Omega = \int_0^{t_H} A e^{[-E_a / RT_H(\tau)]} d\tau = t_H A e^{[-E_a / RT_H]} \quad (3)$$

Of the three studies mentioned, only the first two kept the tissue at a constant temperature during heating, since they used a tissue bath to determine the effect of changing the superfusate temperature [4,5]. In the third, the tissue bath was kept perfused at 37 ºC while heating was induced by gradually increasing RF power, which progressively raised the temperature throughout the entire heating period, thus making it impossible to use Eq. (3). The experimental setup in the first two studies took care to ensure that the tissue temperature rapidly reached the target value (T_H): $t_{1/2}$ (i.e. time required to reach half the value of T_H) was only 0.9±0.3 s in [4] and ~0.75 s in [5], which indicates the appropriateness of Eq. (3) by assuming that the tissue sample was actually subjected to a constant temperature for a fixed time.

Table 1 shows the electrophysiological changes seen in the experimental groups considered in the above-mentioned studies, as well as the Ω values derived from T_H and t_H for each electrophysiological change. The values shown are quite in tune with the value of Ω =1 used in previous computational studies to delineate lesion size: above 0.93 excitability is irreversibly lost, according to Nath *et al* [4] and above 0.77 permanent block occurs according to Simmers *et al* [5]. In the tissue associated with sublethal heating, Ω above 0.1 there would be reversible loss of excitability (with immediate restoration of normal excitability after returning to 37 ºC, according to Nath *et al* [4]), while transient block (absence of impulse conduction for ≤ 5 minutes) occurs above 0.4, according to Simmers *et al* [5]. These two values of 0.1 and 0.4 were assumed to be the lower thresholds to delineate the tissue zone associated with sublethal heating that could cause transient block. The upper threshold was the one due to the permanent block induced by the thermal lesion (i.e. Ω = 1.0). In short, the lesion size will be the one with Ω > 1.0, while the heat-

induced transient block zone will be the one shown by $0.1–0.4 < \Omega < 1.0$ (see Fig. 1). We also checked that the short time the tissue needed to reach the target temperature (T_H) in the experiments [4,5] barely affected the Ω value (e.g. Ω decreases by only 0.02 when t_H is reduced by a couple of seconds).

2.3. Model description

Three-dimensional computational models were built that included a round-tip 7Fr 3.5 mm irrigated electrode placed on the myocardium and surrounded by blood. Three angles were considered between the tissue surface and catheter axis: perpendicular (90º), oblique (45º), and horizontal (0º). Due to the existence of one symmetry plane, the model only considered half of the real volume. We considered electrode insertion depths of 0.5 and 0.7 mm at the 90º angle, mimicking low and medium contact forces [10]. The insertion depths for the other angles were adjusted to keep the contact surface constant, as it is the parameter most closely correlated with the lesion area per ablation [11]. Figure 2 shows the model geometry with the catheter at 45º.

2.4. Ablation protocols

Computer simulations were conducted to model RF delivery at different settings (i.e. combinations of power and pulse duration). The first set of simulations considered three power-duration settings typically used in clinical practice: low power-moderate duration (LPMD, 25 W–20 s) [12], high power-short duration (HPSD, 50 W–6 s) [13] and very high power-very short duration (vHPvSD, 90 W–4 s) [14]. The second set of simulations considered three power-duration settings with energy balanced at 360 J: moderate power-

short duration (LPSD, 30 W−12s), high power-short duration (HPSD, 50 W−7.2 s) and very high power-very short duration (vHPvSD, 90 W−4 s) [7]. The power value used in all the simulations was reduced by 20% as the model did not include the entire torso [15]. The simulation data were obtained for up to 90 s after RF onset to examine the extra lesion growth due to thermal latency [8].

2.5. Tissue properties and governing equations

Tissue properties were taken from the IT'IS Foundation database [16], while the ablation catheter properties were taken from Pérez *et al* [17] (see Table 2). The tissue electrical conductivity was assumed to increase by 1.5%/ºC up to 99 ºC, at which point it decreased by two orders of magnitude (from 99 to 101 ºC) to simulate dehydration by vaporization. The latent heat associated with liquid-to-gas phase change was also considered, assuming the myocardium to have a 70% water content. The models were constructed using the Finite Element Method on ANSYS software (ANSYS, Canonsburg, PA, USA). Laplace's Equation and Bioheat Equation were used to solve the electrical and thermal problem, respectively (see [3] for further details).

A sensitivity analysis was conducted to take into account the dispersion in tissue characteristics, for which we chose the maximum and minimum myocardium values reported in the ITIS database (0.5 and 0.6 W/m·K for thermal conductivity, 1059 and 1143 kg/m^3 for density, 3614 and 3724 J/kg·K for specific heat) [16]. Myocardium and blood electrical conductivity were considered to have a ±10% variation, which is of the same order as the dispersions of the rest of the characteristics, even though the IT'IS database does not include high frequency dispersion (500 kHz). Two very different cases were

considered in terms of energy delivery for the sensitivity analysis: 25 W–20 s and 90 W–4 s (catheter at 90º and 0.5 mm insertion depth). Each model (half of the entire domain, see Fig. 2A) contained of ~220,000 tetrahedral elements and ~300,000 nodes. The outer dimensions (4 cm around the ablation electrode), mesh size (minimum of ~90 μm around the electrode and maximum of ~7 mm in the periphery) and the time step (ranging from 15 to 70 ms) were verified by means of convergence tests.

2.6. Boundary and initial conditions

The power value remained constant during the RF pulse, which meant that both current and voltage were suitably modulated as tissue impedance was gradually reduced. The dispersive electrode was simulated by conditions of 0 V on all the outer surfaces except the symmetry plane. Electrode irrigation was modeled by fixing a value of 25 ºC in the electrode volume not embedded in the tissue and leaving the rest with a free temperature, to mimic a multi-hole electrode, since we assumed that irrigation occupied almost the entire electrode surface [18]. The thermal problem was not solved in the blood, and thermal transfer coefficients for low blood flow condition (0.1 m/s) were used on the electrode-blood and myocardium-blood interfaces instead (3310 $W/m^2 \cdot K$ and 694 $W/m^2 \cdot K$, respectively) to simulate ablation sites with low local blood flow, as in patients with chronic atrial fibrillation and dilated atria [19]. A temperature of 37 ºC was set at the outer contours of the tissue and the initial temperature was also 37 ºC.

2.7. Statistics

This study used a physics-based mechanistic model in which the different factors (catheter orientation, power-duration setting and tissue properties) took different values to simulate a representative sample of what happens during RFCA ablation under varying conditions. The relationships between the variables were studied by simple regression using Excel. Coefficient of determination (R^2) was reported to assess the goodness of fit, along with the p-value (P) to determine statistical significance (calculated by the two-tailed unpaired Student's t test).

3. Results

Figure 3 shows the lesion sizes and of the heat-induced transient block zone with the typical power settings and 0.5 mm insertion depth. The lesion sizes and transient block zones were directly proportional to the energy delivered, with lesion depths of ~3.2 mm at 50W–6s (300 J), ~3.5 mm at 90W–4s (360 J) and ~4.0 mm at 25W–20s (500 J). Overall, the transient block zone extended beyond the lesion limits by between 0.47±0.08 mm and 1.91±0.24 mm in depth, depending on the Ω threshold value considered (0.1 and 0.4, respectively), and between 0.64±0.15 mm and 2.49±0.55 mm in maximum width (see Fig. 3C,D). A strong linear correlation was found between the lesion depth and the depth of the transient block zone (R^2>0.97, P<0.001), while we did not find any statistical significance in the correlation between the maximum width of the lesion and that of the transient block zone.

Figure 4 shows the lesion and transient block zone sizes with the same energy delivery (360 J) and 0.5 mm insertion depth. The lesions were quite similar regardless of the catheter angle and power setting, with mean values of 3.49±0.08 mm in depth and

6.75±0.36 mm in width. The sizes of the transient block zone were also similar at all the catheter angles and power settings, extending beyond the lesion limits by between 0.45±0.02 mm and 1.86±0.05 mm in depth, and between 0.61±0.06 mm and 2.36±0.19 mm in maximum width (see Fig. 4C,D). We found a moderate negative linear correlation between the maximum lesion widths and that of the transient block zone (R^2>0.65–0.72, P<0.05). We did not find a statistically significant correlation between the lesion depths and the transient block zone. For illustrative purposes only, Figure 5 shows temperature progress at depths of 3 and 4.5 mm for three power-duration settings, at a 0.5 mm insertion depth and catheter at 90º. While the 3-mm depth is representative of an area subjected to lethal heating (located within the lesion limits), the 4.5-mm depth is the area exposed to sublethal heating capable to cause transient block.

The results for the 0.7 mm insertion depth showed lesions slightly greater than at 0.5 mm, particularly at depths of ~3.4 mm at 50W–6s (300 J), ~3.7 mm at 90W–4s (360 J) and ~4.2 mm at 25W–20s (500 J). However, the relationship between lesion and transient block zone sizes was almost identical for both insertion depths. The zone of transient block at 0.7 mm insertion and typical power-duration settings extended beyond the lesion limits by between 0.47±0.07 mm and 1.92±0.23 mm in depth (according to the Ω threshold value considered, 0.1 and 0.4, respectively), and between 0.64±0.15 mm and 2.50±0.54 mm in maximum width. The results for 360 J ablations and 0.7 mm insertion were almost identical: 0.45±0.01 mm and 1.87±0.04 mm in depth (according to the Ω threshold value considered, 0.1 and 0.4, respectively) and between 0.61±0.06 mm and 2.37±0.19 mm in maximum width. The dispersion in tissue thermal and electrical characteristics with the size of transient block zone had a moderate impact, since the maximum difference between

using average and maximum/minimum values was less than ±0.3 mm in depth and ±0.5 mm in maximum width.

Figure 6 shows the lesion geometries (Ω=1) and transient block zones (between Ω=1 and Ω=0.1–0.4). Apart from a slight asymmetry of the lesion geometries and the transient block zone with the catheter at 0º, the overall results show that the transient block zone extends between more than 0.5 and 2.0 mm in depth and lesion limits, respectively, regardless of catheter angle.

4. Discussion

4.1. Main findings

An RFCA model was used in this computer study to estimate how far the zone of heat-induced transient block extends beyond the lesion during RF catheter cardiac ablation. While the lesion zone is associated with irreversible loss of electrical impulse conduction characteristics, the transient block zone is associated with transient changes and therefore reversible. An assorted set of real features (such as catheter angle, power-duration setting, electrode insertion depth, dispersion in tissue characteristics) were incorporated into the model to generate applicable results to clinical practice. The study's key findings are as follows:

1) An exact threshold value of the Arrhenius damage index Ω from heat-induced reversible changes cannot be inferred from the few experimental data available, but instead offer a relatively large range, between 0.1 and 0.4.

2) Even taking this relatively large range of Ω values into account, the computer results suggest that the transient block zone extends in depth to at least 0.5 mm and to a maximum of 2 mm outside the lesion limits.

3) The maximum width of the transient block zone seems to vary more with the energy delivered, while the results suggest that it extends beyond the lesion by a minimum of 0.6 mm and a maximum of 2.5 mm, reaching up to 3.5 mm at higher energy settings (25W–20s, 500 J).

4) The dispersion in tissue thermal and electrical characteristics implies the scattering of the size of the transient block zone by ±0.3 mm in depth and ±0.5 mm in maximum width.

Although the existence of a zone peripheral to the RF-induced lesion and affected by transient electrophysiological changes is assumed in RF ablation, since it makes physical sense, there are no previous data that attempt to quantify its size. Our results thus offer this novel information, with important clinical implications for subendocardial ablation targets (i.e. in which the arrhythmic focus is deep), suggesting that when the arrhythmic focus is suspected to be 0.5–2 mm deeper than the lesion limit, a transitory disappearance of the arrhythmia can be expected. In the context of creating linear lesions (e.g. ablation of atrial fibrillation of flutter), our results suggest that two contiguous lesions separated by 1.2–5 mm (i.e. two-fold values of the maximum width of the transient block zone) could temporarily behave like a continuous lesion when in fact there is actually a gap between them.

These estimates are in agreement with the results reported by Simmers *et al* [20], who studied the effects of electrode–target distance and intracavitary blood flow on the

radiofrequency (RF) power required to induce transient conduction block using a Langendorff-perfused canine model, a 7Fr 4-mm standard catheter at 90º (5 g contact force) and 0.15 m/s blood flow. They found that 3 and 7 W were required to produce transient conduction block at 0 and 2 mm from the electrode, while it was not possible to induce block at 4 mm due to the RF power required being such that its delivery was terminated prematurely by a sudden impedance rise and coagulum formation at the catheter tip. Although neither the conditions nor the objective of the study by Simmers *et al* [20] were exactly like ours, their results suggest that the sublethal heating zone causing a transient block could reach 2 mm, but never 4 mm. It should be noted that our results suggest a range of 0.6–2.5 mm in terms of width and that Simmers *et al* [20] changed the distance between the RF catheter and the point at which transient block was assessed by moving the catheter over the tissue surface.

4.2. Experimental validation of the heat-induced transient block zone model

The ability of the current computational models to predict temperature maps and lesion size during RFCA has been extensively demonstrated, with errors of $< 3 - 7$ ºC for tissue temperature at > 3 mm deep and 1–2 mm in terms of lesion size [3]. We therefore focused on checking how our proposed transient block model (described in Section 2.2) is consistent with the results obtained in preclinical studies, especially those based on ex vivo models that measure the intramyocardial temperature progress at different depths below the electrode (e.g. [21–23]). In theory, from this data we could determine the 'thermal history' associated with each point and so calculate the Ω value by Eq. (2). If this information is

crossed with the lesion size reported in the same studies, it might be possible to identify the points in the tissue subjected to lethal heating capable to cause transient block.

As a simple illustration to emphasize how Eq. (2) can compute the damage index Ω, we chose the temperature measurements obtained by Demazumder *et al* [21] at 3, 5 and 7 mm, in particular the four experimental groups that included blood flow around the electrode (Groups 2, 4, 6 and 8, see Table 3). If we now simplify the temperature progress to a linear rise during the RF pulse (as has been reported) and a four times slower drop after the pulse, then we can apply Eq. (2) to estimate the Ω value in each group and depth (see Table 3). Overall, we found that the Ω values obtained were consistent with the lesion sizes reported for each group.

For instance, in Group 2, where lesion depth was 4.2±0.3 mm, the Ω value at 3 mm deep was 0.938, i.e. almost 1, which represents the irreversibly damaged tissue. In contrast, at 5 mm the Ω value was 0.091, i.e. almost 0.1, which can be expected, since 5 mm is ~1 mm beyond the lesion limit, i.e. the sublethal heating zone (note that our results suggest a range of 0.5–2.5 mm). At 7 mm, i.e. ~3 mm beyond the lesion limit, Ω =0.021, which is much lower than 0.1 and thus is at a point outside the sublethal heating zone.

In Group 4 the Ω value at 3 mm was ~9.1 (much higher than 1.0), which is consistent with the fact that the lesion limit is really 2 mm deeper (5 mm). The Ω value at 5 mm was 0.314, which in our model was in the sublethal heating zone and agrees with the fact that lesion depth is just around 5.0 mm (±1.0 mm). The Ω value at 7 mm was 0.126, which is associated with sublethal heating at a distance of ~2 mm from the lesion limit. In the

remaining cases (Groups 6 and 8) the Ω values were much higher than 1.0 at 3, 5 and 7 mm deep, since all these points were within the lesion boundary (8 mm).

In terms of clinical impact, we must recognize that the most important issue in the context of RFCA modeling is to predict the lesion size, i.e. the tissue volume delimited by Ω>1. Although the main efforts have to be hence centered on optimizing the RF pulse parameters to increase the lesion size, we think that knowledge about how large the periablational zone responsible of transient block is worthy scientific information in the context of cardiac electrophysiology.

4.3. Limitations

The threshold Ω values used to determine the transient block zone were obtained from only two experimental studies and only 2 different heating durations (30 s [5] and 60 s [4]). One might wonder to what extent the Arrhenius function is valid for shorter exposure times, such as those associated with high-power short-duration (HPSD) ablation. In this regard, Simmers *et al* [5] evaluated the electrophysiological changes in transient block not only at 30 s but at 0, 10, 20 and 30 s heating durations, and found a progressive drop in all the variables leading up to a transient block (including conduction velocity), which suggests that the combined effect of temperature and duration might be the key factors in the changes associated with reversible block and not just the threshold temperature. This was also confirmed by Cote *et al* [24], who found that time to transient block during the application of low-temperature short-duration RF pulses was significantly longer for 50 ºC applications than 70 ºC applications on the same site. The limitations inherent in the two experimental studies should also be considered: *in vitro* pig [4] and a canine [5] model,

with only ventricular samples. In this regard, the great complexity of conducting this type of experimental study on human tissue under *in vivo* conditions should be recognized, in the same way that it would be very complex to experimentally assess the extension of the reversible block zone. Our results based on an *in silico* model certainly have many limitations, but they represent the first estimate made to date.

By assuming that the sublethal heating zone capable to cause transient block is the one with Ω values between 0.1–0.4 and 1.0, we are really using the Arrhenius thermal injury index Ω to model the transient electrophysiological changes induced by heating, not the irreversible thermal damage (lesion size), so that the percentage of living cells as expressed in Eq. (1) is a meaningless parameter in our case. This limitation comes from the fact that specific values of A and E_a are not available for modeling the transient electrophysiological changes induced by moderate heating in the myocardium.

Our mathematical model was only based on the electrophysiological changes associated with a 'progressive loss' of electrical activity (excitability in Nath *et al* [4] and block in Simmers *et al* [5]). We did not consider the increasing conduction velocity found in the latter case [5], when the tissue was subjected to very mild heating: from 38.5 to 45.4 ºC for 30 s, which is equivalent to Ω values ranging from 0.01 to 0.12, according to Eq. (3). This assumption was made since we were only interested in estimating the size of the zone with RF-induced electrophysiological behavior similar to that of an ablated zone, which should itself manifest as a loss in excitability and block. It is also important to point out that the Arrhenius function only considered the RF-induced acute changes, and that hence late electrophysiological effects due for instance to microvascular injury [25] might occur beyond the region of acute coagulation necrosis, causing the extension of the lesion.

Despite the fact that only a rounded-tip 7Fr 3.5 mm catheter was considered, previous results have shown that both flat-tip and round-tip catheter lesions are quite similar [7]. Neither is there any reason to assume that the relationship between lesion size and the transient block zone will be different when the electrode size varies slightly within the margins of the currently available catheters (7–8 Fr in diameter, 3–4 mm in length). Likewise, the fact that the model did not include other features (such as multi-parameter indexes –e.g. ablation index AI and lesion index LSI– and different blood flow rates) does not seem to affect the estimation of the relative size of the transient block zone in relation to lesion size.

Although the model assumed a homogeneous tissue instead of an arrangement based on different tissue layers (myocardium, epicardial fat, connective tissue, etc), it had already been found that this has little impact in terms of lesion depth [7] and there is no physical reason to think that something different will happen with the transient block zone size. Finally, we did not consider extreme cases in which considerable energy is delivered, e.g. power $\geq$ 30 W or repetitive applications on the same point [26], which we must recognize as being able to change the relative relationship between lesion size and the transient block zone.

5. Conclusions

Using a mathematical model based on the assumption that the sublethal heating zone capable to cause transient block is that of Arrhenius index values between 0.1 and 0.4, our simulation results suggest that the transient block zone might extend beyond the lesion limit by between 0.5 and 2 mm in depth and between 0.6 and 2.5 mm in maximum width. A

±10% dispersion in the tissue characteristics would have a moderate impact on these dimensions (±0.3 mm in depth and ±0.5 mm in maximum width).

References

1. Viglianti BL, Dewhirst MW, Abraham JP, Gorman JM, Sparrow EM. Rationalization of thermal injury quantification methods: application to skin burns. Burns. 2014 Aug;40(5):896-902. doi: 10.1016/j.burns.2013.12.005.
2. Haines DE. Letter by Haines regarding article, "Direct measurement of the lethal isotherm for radiofrequency ablation of myocardial tissue". Circ Arrhythm Electrophysiol. 2011 Oct;4(5):e67; author reply e68. doi: 10.1161/CIRCEP.111.965459.
3. González-Suárez A, Pérez JJ, Irastorza RM, D'Avila A, Berjano E. Computer modeling of radiofrequency cardiac ablation: 30 years of bioengineering research. Comput Methods Programs Biomed. 2022 Feb;214:106546. doi: 10.1016/j.cmpb.2021.106546.
4. Nath S, Lynch C 3rd, Whayne JG, Haines DE. Cellular electrophysiological effects of hyperthermia on isolated guinea pig papillary muscle. Implications for catheter ablation. Circulation. 1993 Oct;88(4 Pt 1):1826-31. doi: 10.1161/01.cir.88.4.1826.
5. Simmers TA, De Bakker JM, Wittkampf FH, Hauer RN. Effects of heating on impulse propagation in superfused canine myocardium. J Am Coll Cardiol. 1995 May;25(6):1457-64. doi: 10.1016/0735-1097(94)00559-9.
6. Simmers TA, de Bakker JM, Wittkampf FH, Hauer RN. Effects of heating with radiofrequency power on myocardial impulse conduction: is radiofrequency ablation exclusively thermally mediated? J Cardiovasc Electrophysiol. 1996 Mar;7(3):243-7. doi: 10.1111/j.1540-8167.1996.tb00521.x.
7. Pérez JJ, D'Angelo R, González-Suárez A, Nakagawa H, Berjano E, d'Avila A. Low-energy (360 J) radiofrequency catheter ablation using moderate power - short duration: proof of concept based on in silico modeling. J Interv Card Electrophysiol. 2022 Jul 7. doi: 10.1007/s10840-022-01292-z.
8. Irastorza RM, d'Avila A, Berjano E. Thermal latency adds to lesion depth after application of high-power short-duration radiofrequency energy: Results of a computer-modeling study. J Cardiovasc Electrophysiol. 2018 Feb;29(2):322-327. doi: 10.1111/jce.13363.
9. Pearce JA. Comparative analysis of mathematical models of cell death and thermal damage processes. Int J Hyperthermia. 2013 Jun;29(4):262-80. doi: 10.3109/02656736.2013.786140.
10. Pérez JJ, Nadal E, Berjano E, González-Suárez A. Computer modeling of radiofrequency cardiac ablation including heartbeat-induced electrode displacement. Comput Biol Med. 2022 May;144:105346. doi: 10.1016/j.compbiomed.2022.105346.
11. Masnok K, Watanabe N. Catheter contact area strongly correlates with lesion area in radiofrequency cardiac ablation: an ex vivo porcine heart study. J Interv Card Electrophysiol. 2022 Apr;63(3):561-572. doi: 10.1007/s10840-021-01054-3.
12. Kotadia ID, Williams SE, O'Neill M. High-power, Short-duration Radiofrequency Ablation for the Treatment of AF. Arrhythm Electrophysiol Rev. 2020 Feb 12;8(4):265-272. doi: 10.15420/aer.2019.09.
13. Barbhaiya CR, Kogan EV, Jankelson L, et al. Esophageal temperature dynamics during high-power short-duration posterior wall ablation. Heart Rhythm. 2020 May;17(5 Pt A):721-727. doi: 10.1016/j.hrthm.2020.01.014.
14. Kotadia ID, Williams SE, O'Neill M. High-power, Short-duration Radiofrequency Ablation for the Treatment of AF. Arrhythm Electrophysiol Rev. 2020 Feb 12;8(4):265-272. doi: 10.15420/aer.2019.09.
15. Irastorza RM, Gonzalez-Suarez A, Pérez JJ, et al. Differences in applied electrical power between full thorax models and limited-domain models for RF cardiac ablation. Int J Hyperthermia. 2020;37(1):677-687. doi: 10.1080/02656736.2020.1777330.
16. Hasgall PA, Di Gennaro F, Baumgartner C, Neufeld E, Lloyd B, Gosselin MC, Payne D, Klingenböck A, Kuster N. IT'IS Database for Thermal and Electromagnetic Parameters of Biological Tissues, Version 4.1, Feb 22, 2022, doi: 10.13099/VIP21000-04-1. itis.swiss/database (accessed 2 October 2022).
17. Pérez JJ, Ewertowska E, Berjano E. Computer modeling for radiofrequency bipolar ablation inside ducts

and vessels: relation between pullback speed and impedance progress. Lasers Surg Med. 2020 Nov;52(9):897-906. doi: 10.1002/lsm.23230.
18. González-Suárez A, Pérez JJ, Berjano E. Should fluid dynamics be included in computer models of RF cardiac ablation by irrigated-tip electrodes? Biomed Eng Online. 2018 Apr 20;17(1):43. doi: 10.1186/s12938-018-0475-7.
19. Nakagawa H, Ikeda A, Sharma T, Govari A, Ashton J, Maffre J, Lifshitz A, Fuimaono K, Yokoyama K, Wittkampf FHM, Jackman WM. Comparison of In Vivo Tissue Temperature Profile and Lesion Geometry for Radiofrequency Ablation With High Power-Short Duration and Moderate Power-Moderate Duration: Effects of Thermal Latency and Contact Force on Lesion Formation. Circ Arrhythm Electrophysiol. 2021 Jul;14(7):e009899. doi: 10.1161/CIRCEP.121.009899.
20. Simmers TA, de Bakker JM, Coronel R, Wittkampf FH, van Capelle FJ, Janse MJ, Hauer RN. Effects of intracavitary blood flow and electrode-target distance on radiofrequency power required for transient conduction block in a Langendorff-perfused canine model. J Am Coll Cardiol. 1998 Jan;31(1):231-5. doi: 10.1016/s0735-1097(97)00435-x.
21. Demazumder D, Mirotznik MS, Schwartzman D. Comparison of irrigated electrode designs for radiofrequency ablation of myocardium. J Interv Card Electrophysiol. 2001 Dec;5(4):391-400. doi: 10.1023/a:1013241927388. PMID: 11752907; PMCID: PMC5779084.
22. Demazumder D, Mirotznik MS, Schwartzman D. Biophysics of radiofrequency ablation using an irrigated electrode. J Interv Card Electrophysiol. 2001 Dec;5(4):377-89. doi: 10.1023/a:1013224110550. PMID: 11752906; PMCID: PMC5779086.
23. Wong WS, VanderBrink BA, Riley RE, Pomeranz M, Link MS, Homoud MK, Estes NA 3rd, Wang PJ. Effect of saline irrigation flow rate on temperature profile during cooled radiofrequency ablation. J Interv Card Electrophysiol. 2000 Apr;4(1):321-6.
24. Cote JM, Epstein MR, Triedman JK, Walsh EP, Saul JP. Low-temperature mapping predicts site of successful ablation while minimizing myocardial damage. Circulation. 1996 Aug 1;94(3):253-7. doi: 10.1161/01.cir.94.3.253.
25. Nath S, Whayne JG, Kaul S, Goodman NC, Jayaweera AR, Haines DE. Effects of radiofrequency catheter ablation on regional myocardial blood flow. Possible mechanism for late electrophysiological outcome. Circulation. 1994 Jun;89(6):2667-72. doi: 10.1161/01.cir.89.6.2667.
26. Sánchez-Muñoz EJ, Berjano E, González-Suárez A. Computer simulations of consecutive radiofrequency pulses applied at the same point during cardiac catheter ablation: Implications for lesion size and risk of overheating. Comput Methods Programs Biomed. 2022 Jun;220:106817. doi: 10.1016/j.cmpb.2022.106817.

Table 1. Relation between electrophysiological changes observed in previous experimental studies and the *in silico* model parameters.

Previous experimental studies				***In silico* model parameters**
Study	**t_H (s)**	**T_H (ºC)**	**Electrophysiological change**	**Ω value [1]**
Nath *et al* [4]	60	42.7–51.3 ºC (median 48.0 ºC)	Reversible loss of excitability	**0.10**–1.37 (median 0.51)
		≥ 50 ºC	Irreversible loss of excitability	≥ 0.93
Simmers *et al* [5]	30	49.5–51.5 ºC	Transient block	**0.40**–0.73
		51.7–54.4 ºC	Permanent block	0.77–1.70

t_H: Heating duration; T_H: Temperature. [1]Computed from Eq. (3) using t_H and T_H values. In **bold** the values assumed as the lower threshold of the tissue zone subjected to transient electrophysiological changes induced by sublethal heating (the upper threshold was the one corresponding to irreversible changes, i.e. thermal lesion Ω = 1.0).

Table 2. Characteristics of tissues and materials of each element used in the models [16,17].

Element/Material	**σ (S/m)**	**k (W/m·K)**	**ρ (kg/m^3)**	**c (J/kg·K)**
Electrode/Pt-Ir	4.6×10^6	71	21500	132
Catheter/Polyurethane	10^{-5}	23	1440	1050
Cardiac Chamber/Blood	0.748	--	--	--
Fat (average infiltrated)	0.0438	0.21	911	2348
Connective	0.391	0.39	1027	2372
Myocardium	0.281	0.56	1081	3686

σ, electrical conductivity (at 500 kHz); k, thermal conductivity; ρ, density; and c, specific heat (all assessed at 37 ºC in case of tissue and blood).

Table 3. Summary of the results reported by Demazumder *et al* [21] for eight experimental groups and Ω values computed using the Eq. (2).

Groups	**t_{RF} (s)**	**$T_{3\text{-mm}}$**	**$\Omega_{3\text{-mm}}$**	**$T_{5\text{-mm}}$**	**$\Omega_{5\text{-mm}}$**	**$T_{7\text{-mm}}$**	**$\Omega_{7\text{-mm}}$**	**D (mm)**
2	15±2	57±7	0.938*	47±3	0.091**	39±3	0.021	4.2±0.3
4	32±16	65±14	9.088	51±12	0.314	47±6	0.126	5.0±1.0
6	60±0	92±3	8900	81±5	750	67±6	28	7.6±0.8
8	60±0	96±4	21,300	81±6	750	66±6	22	8.0±0.0

t_{RF}: RF duration; $T_{X\text{-mm}}$: Maximum temperature reached at the end of the RF pulse at the depth X; D: lesion depth; *Approximately 1.0; ** Approximately 0.1.

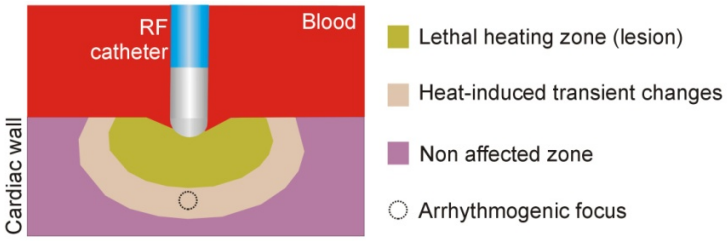

Figure 1 RF-induced lesion groups those cardiac cells that have been subjected to a lethal thermal dose which has resulted in irreversible changes in their electrical activity (e.g. irreversible loss of excitability and block). Around, other cells have been subjected to sublethal (moderate) heating, with the consequent transient electrical change (e.g. reversible loss of excitability and block) [4,5]. Further on are those cells that have been subjected to much milder heating and have also temporarily increased their rate of electrical conduction [4], and finally cells that have not undergone temperature-induced changes since their temperature hardly changed during RFCA.

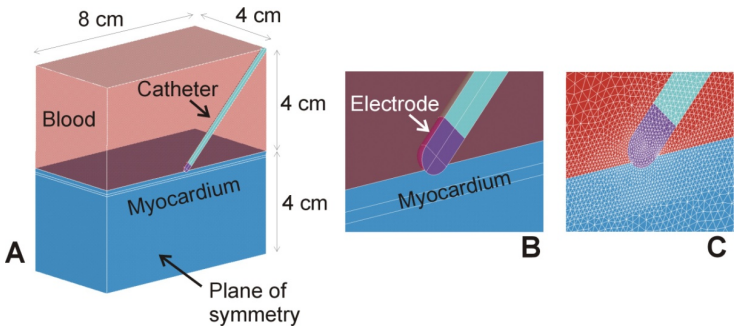

Figure 2. **A:** 3D model geometry for the case of oblique catheter orientation. **B**: Detail of the electrode-myocardium contact. **C**: Detail of the meshing around the electrode.

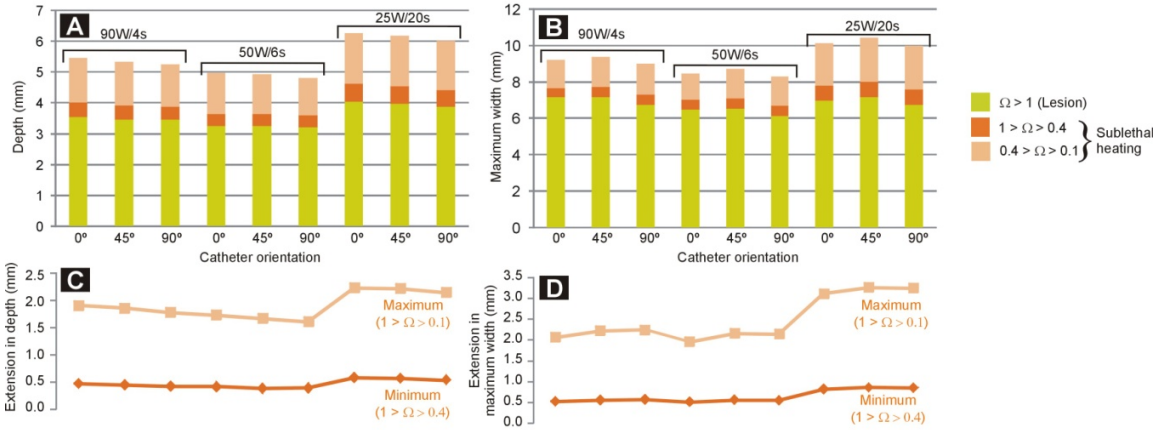

Figure 3 Depth (**A**) and maximum width (**B**) of lesion and transient block zone for three catheter orientation (perpendicular 90º, oblique 45º and horizontal 0º) and different power-duration settings. Extension in depth (**C**) and maximum width (**D**) of the transient block zone beyond the lesion contour.

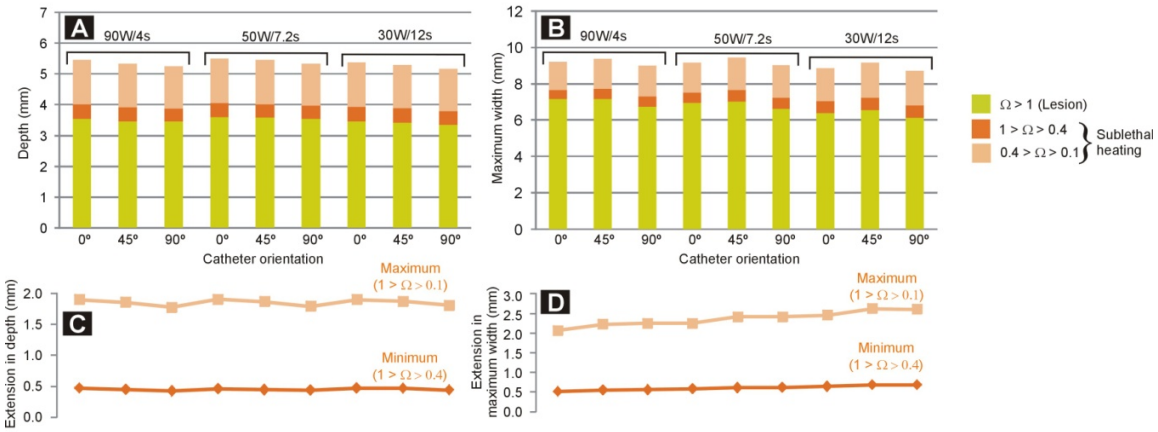

Figure 4 Depth (**A**) and maximum width (**B**) of lesion and transient block zone for three catheter orientation (perpendicular 90º, oblique 45º and horizontal 0º) and power-duration settings delivering the same energy (360 J). Extension in depth (**C**) and maximum width (**D**) of the transient block zone beyond the lesion contour.

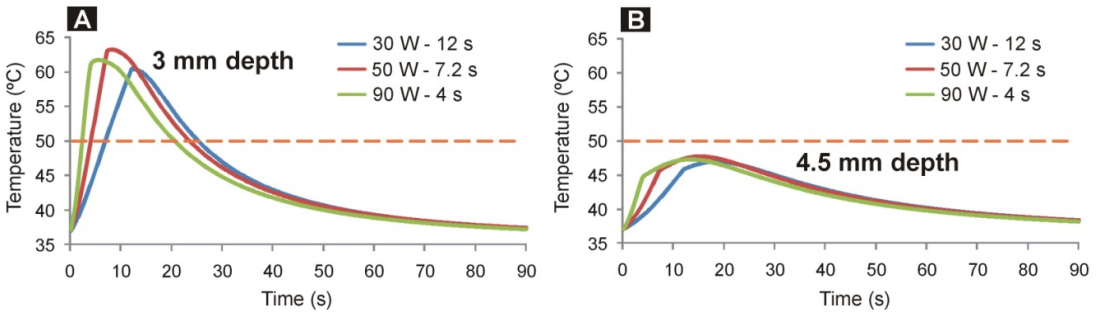

Figure 5 Temperature progress of the temperature at 3 and 4.5 mm depths during and after the RF pulse in case of perpendicular catheter (0º orientation) and three power-duration settings. Dashed line corresponds with the 50 ºC isotherm (usually considered as the lethal threshold).

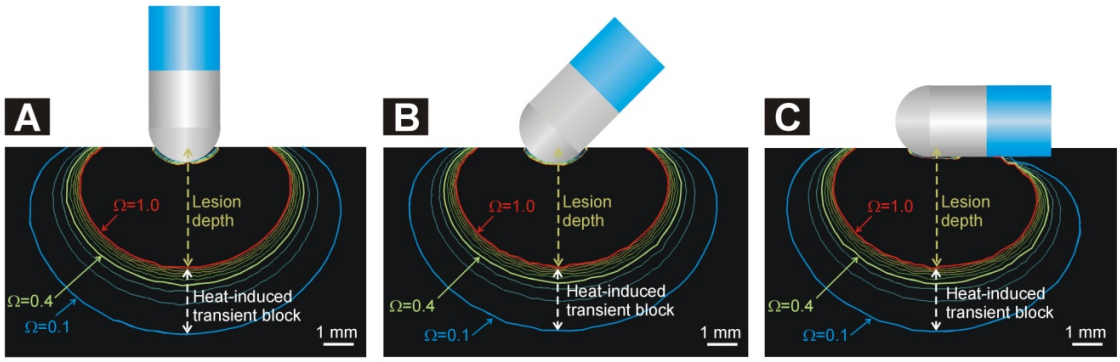

Figure 6 Distributions of the Ω value at 90 s for 25W–20s RFCA (0.5 mm insertion depth) at different catheter orientations: perpendicular (**A**), oblique (**B**) and parallel (**C**). Tissue points within the Ω=1 isoline represent irreversible damaged zone (lesion), while the transient block zone would extend to at least Ω=0.4 and at most to Ω=0.1.